Food Chemistry 138 (2013) 2195–2200

Contents lists available at SciVerse ScienceDirect

Food Chemistry

journal homepage: www.elsevier.com/locate/foodchem

Analytical Methods

Application of reduced graphene oxide and carbon nanotube modified electrodes for measuring the enzymatic activity of alcohol dehydrogenase

Xianlong Wang [a,b], Li Li [c], Yanping Wang [a], Chongzheng Xu [a], Bo Zhao [a,*], Xiaodi Yang [a,*]

[a] Jiangsu Key Laboratory of New Power Batteries, School of Chemistry and Materials Science, Nanjing Normal University, Nanjing 210097, China
[b] Key Laboratory of NeuroInformation of Ministry of Education, Center of Bioinformatics, University of Electronic Science and Technology of China, Chengdu 610054, China
[c] School of Biochemical and Environmental Engineering, Nanjing Xiaozhuang University, Nanjing 211171, China

ARTICLE INFO

Article history:
Received 30 August 2012
Received in revised form 28 November 2012
Accepted 30 November 2012
Available online 28 December 2012

Keywords:
Aluminium
Al_{13}
Alcohol dehydrogenase
Nicotinamide adenine dinucleotide

ABSTRACT

An electrochemical method was developed to measure the enzymatic activity of alcohol dehydrogenase (ADH) by monitoring the amount of reduced nicotinamide adenine dinucleotide (NADH) generated in the catalysed oxidation of ethanol by ADH. The concentration of NADH was determined by amperometric measurements, which recorded the oxidation current of NADH versus time on reduced graphene oxide and functionalised multi-walled carbon nanotube modified electrodes. The initial reaction rates and the apparent Michaelis constants of the enzymatic reaction were obtained in the absence and presence of Al^{3+} and nanometre-sized tridecameric aluminium polycationic (nano-Al_{13}) species. The results showed that Al^{3+} and nano-Al_{13} exhibited inhibitory effect on the enzymatic activity of ADH. Fluorescence and circular dichroism spectra indicated the inhibitory effect was likely caused by the conformational changes of ADH and/or NADH induced by Al^{3+} and nano-Al_{13}.

1. Introduction

Alcohol dehydrogenases (ADH) are a family of dehydrogenase enzymes that catalyse the interconversion between alcohols and aldehydes or ketones. ADH is widely distributed in the liver of humans and animals, plants and microbial cells. Yeast ADH is a well-known Zn-containing metalloenzyme catalysing the last step of the fermentation reaction of ethanol to acetaldehyde (Ramaswamy et al., 1994). This crucial enzyme has been well studied for its applications in wine and beer production and biotechnological processes for the bioconversion of different organic wastes into ethanol (Lortie, Fassouane, Laval, & Bourdillon, 1992). The oxidation reactions catalysed by ADH are coupled with the reduction of the coenzyme nicotinamide adenine dinucleotide (from the oxidised form, NAD^+, to the reduced form, NADH). Our previous studies showed that Al(III) displays strong complexation ability with both NAD^+ and NADH (Yang, Zhang, Li, & Shen, 2007). Therefore, Al(III) species may exert interference on the catalytic activity of the coenzyme NAD^+-dependent enzymes. In this work, we used ADH as a model enzyme system to demonstrate such an effect. Interestingly, Copeland and De Lima (1992) found that Al(III) inhibited the growth of wheat roots in acidic soils, but the specific activity of ADH was significantly increased and the effect was induced by concentrations of Al(III) as low as 15 μM in the nutrient medium. The authors speculated the increase of the specific activity of ADH may have been due to enhanced expression of the enzyme. The direct effect of Al(III) to the enzyme's activity remains to be understood.

Aluminium has been known as a neurotoxic agent to experimental animals since the last century (Exley, Price, & Birchall, 1994). It is also known as an important relevant aetiological factor in several diseases, such as dialysis treatment, Alzheimer's disease, Parkinson's disease, osteomalacia and anaemia (Orihuela, Meichtry, & Pizarro, 2005). It is not only present in soil, minerals, rocks and water, but may also be naturally present in food, or introduced through additives or the contact with food packaging machines, containers, aluminium foil or kitchen utensils containing this metal (Soni, White, Flamm, & Burdock, 2001). In addition, some Al(III) compounds are used as a flocculent in water treatment. Recent *in vitro* studies demonstrated that Al(III) could inhibit the activity of the enzymes which catalyse the tricarboxylic acid cycle and the glycolytic cycle (Auger, Lemire, Cecchini, Bignucolo, & Appanna, 2011; Sánchez-Iglesias et al., 2009).

Nanotechnology has attracted considerable attention in the scientific community since its emergence as a powerful basic and applied science tool. The potential effects of nanoparticles which lead to unforeseen health or environmental hazards to human beings

Abbreviations: ADH, alcohol dehydrogenases; NAD^+, nicotinamide adenine dinucleotide; NADH, nicotinamide adenine dinucleotide; rGO, reduced graphene oxide; MWNT, multi-walled carbon nanotube; CHIT, chitosan; TEM, transmission electron microscopy.

* Corresponding authors. Tel.: +86 25 83598648; fax: +86 25 85891767.
E-mail addresses: zhaobo@njnu.edu.cn (B. Zhao), yangxiaodi@njnu.edu.cn (X. Yang).

0308-8146/$ - see front matter © 2012 Elsevier Ltd. All rights reserved.
http://dx.doi.org/10.1016/j.foodchem.2012.11.137

and other species have raised considerable concerns. There are many studies on the toxicity of nanomaterials, such as fullerene and its derivatives, quantum dots and nano-oxides (titania, silica, zinc oxide, alumina, etc.) (Dunphy Guzmán, Taylor, & Banfield, 2006). As a new type purification agent, nanometre-sized tridecameric aluminium polycation (nano-Al_{13}, also called nano-polynuclear Al_{13}) is an effective coagulation agent with rapid aggregation rate over a relatively wide range of pH, and has been widely applied in water treatment. Nano-Al_{13} is also used in a number of other commercial products, such as pillaring agents, antacids, antiperspirants and surface active agents (Casey, 2006). It has been reported that nano-Al_{13} is probably the major species of aluminium under physiological conditions, and the process of $Al(OH)_3$ formation requires the presence of nano-Al_{13} as a precursor. Rao and Rao (1992) found the presence of the Al_{13} species inside synaptosomes. Al_{13} was found to show 10-fold toxicity to plant root relative to the monomeric Al(III) species and comparable toxicity to algae as the monomeric Al(III) species (Furrer, Phillips, Ulrich, Pöthig, & Casey, 2002). Therefore, researchers have paid attention to the toxicity of Al_{13} towards the activity of proteins and enzymes at a molecular level.

In this study, we applied electrochemical methods to investigate how the aqueous Al^{3+} and Al_{13} species affect the catalytic activity of ADH under physiological conditions. In the past few decades, electrochemical methods have been used to study the effect of metal ions on the activity of dehydrogenases (Yang, Li, & Bi, 2005). The inhibitory effect of a number of regulators, such as metal cations (Yin et al., 2010), anticancer antibiotics, mithramycin and chromomycin A_3 (Devi, Chakraborty, & Dasgupta, 2009), on the activity of ADH from various organisms has been studied. However, there has been no study on the effect of aqueous Al(III) species on the enzymatic activity of ADH except for the study of Copeland, & De Lime, (1992) which found Al(III) in a nutrient medium led to increased specific activity of ADH in wheat roots. Although Al(III) is redox inert under normal aqueous electrochemical measurement conditions, NADH can be readily oxidised and the effect of Al(III) species can be monitored by measuring the oxidation current of the coenzyme. However, the oxidation potential of NADH on a bare electrode, such as gold or glassy carbon electrode, is too high, in the range of 0.55–0.85 V (Saleh, Rahman, Okajima, Mao, & Ohsaka, 2011; Yuan, Chen, Wu, Fang, & Niu, 2011). Many other molecules, e.g., catecholamine, ascorbic acid and urea, will be oxidised as well (Gorton & Domínguez, 2002). Furthermore, NAD^+ and the side-reaction products may adsorb on the electrode and reduce the measurement quality. To circumvent these problems, we chose reduced graphene oxide and multi-walled carbon nanotubes to modify the glassy carbon electrode for electrochemical measurements.

Carbon nanomaterials, a large and important family of nanomaterials with advantageous thermal, electrical, mechanical properties, have been widely used as carbon electrodes in electrochemical studies (Zhou, Zhai, & Dong, 2009). Graphene is a recently discovered two-dimensional carbon sheet.

In this work, we developed an electrochemical method based on reduced graphene oxide and carbon nanotube modified electrodes to detect the oxidation current of NADH at a lower potential and applied it to measure the enzymatic activity of ADH in the presence of Al^{3+} and Al_{13} species.

2. Experimental

2.1. Materials and instrumentation

Alcohol dehydrogenase (ADH, EC 1.1.1.1) from yeast, nicotinamide adenine dinucleotide in reduced and oxidised forms (NADH and NAD^+) were purchased from Sigma–Aldrich Co. (St. Louis, MO). Multi-walled carbon nanotube (MWNT, <10 nm in diameter and 0.5–500 nm in length with purity of >95%) was purchased from Shenzhen Nanotech Port Co., Ltd. (Shenzhen, China). All other chemicals were of analytical reagent grade. All solutions were prepared with double-distilled water (ddH_2O). Tris–HCl buffer solution was prepared by dissolving the appropriate amount of Tris(hydroxymethyl)aminomethane, and then adjusting pH using concentrated hydrochloric acid. Aluminium stock solution was prepared by dissolving high purity metallic Al powder (99.99%) in hydrochloric acid at pH < 2 to prevent the hydrolysis of Al^{3+} ion. The stock solution was diluted using ddH_2O.

Electrochemical measurements were performed using a model CHI660B electrochemical station (CH Instruments, Chenhua Inc., Shanghai, China). A three-electrode configuration was employed, which consists of a bare or modified electrode as working electrode, a platinum wire and a saturated calomel electrode as auxiliary and reference electrodes, respectively. Before each electrochemical experiment, the solution was degassed for at least 20 min by bubbling high-purity nitrogen gas, and a nitrogen environment was then kept over the solution during the whole experimental period. The fluorescence spectra were measured on a model LS-50B spectrofluorimeter (Perkin–Elmer, Waltham, MA). The circular dichroism spectra were measured on a Chirascan spectrometer (Applied Photophysics, Leatherhead, UK).

2.2. Preparation of the modified electrodes

A glassy carbon electrode was successively polished on a mirror finish using 0.3 and 0.05 μm alumina slurry and then rinsed thoroughly with ddH_2O. After successive sonications in absolute alcohol and ddH_2O, the electrode was rinsed with ddH_2O and allowed to dry at room temperature.

Graphene oxide (GO) was prepared from natural graphite powder, potassium permanganate, sulphuric acid and sodium nitrate, using a modified Hummers method (Kovtyukhova et al., 1999). The GO product was dispersed in water with the ultrasonic dispersing method to prepare 1 mg/mL GO brown suspension (Ma, Liu, Tang, Yin, & Ai, 2011; Zhu, Chen, & Yang, 2010). A 1.0 wt.% chitosan (CHIT) stock solution was prepared by dissolving chitosan flakes in a hot (80–90 °C) aqueous solution of 1% acetic acid. The solution was cooled to room temperature, and its pH was adjusted to 3.5–5.0 using a concentrated NaOH solution. The CHIT solution was added into the above GO suspension to form a homogenous dispersion. To prepare the GO modified electrode, 4 μL GO/CHIT solution were cast onto the polished electrode and dried at room temperature for 8 h. In order to obtain the reduced graphene oxide (rGO) modified electrode, hydrazine hydrate was added into a centrifuge tube with a GO modified electrode inside, and heated for 6 h at 80 °C.

The MWNT modified electrode was prepared as in our previous studies (Cai et al., 2010). Experimental results showed that the modified electrodes displayed excellent stability, sensitivity and analytical performance for the determination of NADH.

2.3. Synthesis of nano-polynuclear aluminium sulphate

Twenty-five millilitres of 0.25 M aluminium chloride solution were heated and kept at 70 °C using a thermostat. Then, 60 mL of 0.25 M NaOH solution were slowly added under continuous stirring with accurate rate control. After the obtained solution was kept for 24 h at room temperature, 62.5 mL of 0.1 M Na_2SO_4 solution were added. After 10 min, the solution was filtered and aged for 48 h. The crystal obtained from the centrifugalisation was washed twice using ddH_2O and 70% ethanol solution, respectively, then air-dried and stored in a desiccator for future use. The X-ray

diffraction pattern and the nuclear magnetic resonance spectra of the obtained crystal were in good agreement with previous reports (Hu, Liu, & Qu, 2005; Shi, Li, Wang, & Tang, 2007), which showed that nano-polynuclear aluminium sulphate has been successfully synthesised.

3. Results and discussion

3.1. Characterisation of the reduced graphene oxide and MWNT

The graphene oxide (GO) and MWNT were characterised by transmission electron microscopy (TEM) and the images are given in the Supplemental Data. The graphene oxide exhibited transparent and drape film morphology. The intrinsic wrinkled shape of GO is beneficial in maintaining a large surface area on the modified electrode since the structure cannot collapse back to the graphite structure.

The modified electrodes were characterised by Fourier-transform infrared (FT-IR) spectroscopy and the spectra are given in the Supplemental Data. The absorption bands around 3400, 1731, 1630, 1412, 1220 and 1047 cm^{-1} in the spectrum of GO are due to the vibrational modes of the oxygen-containing functional groups on GO (Zhou et al., 2009). After the reduction, only a small amount of residual oxygen was still present on the rGO surface. The MWNT modified electrode displayed feature peaks corresponding to the oxygen-containing functional groups, which demonstrated these groups were successfully introduced (Cai et al., 2010).

3.2. Electrochemical response of NADH on the modified electrodes

On the bare glassy carbon electrode, the cyclic voltammograms of 0.3 mM NADH in 0.1 M tris–HCl buffer (pH 7.5) solution showed that the oxidation current peak of NADH appeared at 0.65 V (Fig. 1A). On the rGO and MWNT modified electrodes, the oxidation peak potential shifted to 0.37 and 0.30 V, respectively (Fig. 1B and C). The shift of the oxidation potential to the lower values suggests the modification layer accelerates the electron transfer from the adsorbed molecules to the electrodes. The wide oxidation peak at *ca.* 0.1 V on the rGO modified electrode was possibly due to the quinone-like moieties on the reduced graphene sheet (Wang et al., 2009). A similar peak also appeared at *ca.* −0.1 V on the MWNT modified electrode, which characterised the oxidation of the oxygen-containing functional groups on the surface of the nanotube. Both the modified electrodes are effective in lowering the oxidation potential of NADH.

The modified electrodes showed good stability. After 50 successive scans, there was only 4% loss of the peak current. After the modified electrodes were stored on a shelf for 3 weeks, there was about 8% loss of the peak current.

The amperometric measurements were used to record the oxidation current of NADH. For the measurements on the rGO modified electrode, the potential was fixed at 0.37 V, and on the MWNT-modified electrode the potential was fixed at 0.30 V. The oxidation current, *i*, was recorded versus time, *t*. A same amount of NADH was continuously added into a tris–HCl buffer solution at pH 7.5 after a fixed time interval (~50 s). The oxidation current reached a constant value within 5 s after each addition of NADH which indicated a quick response of the electrodes to the concentration change. The recorded current increased gradually as more NADH was added and it showed a good linear correlation with the concentration of NADH. Therefore, the amperometric measurements using the modified electrodes could be used to determine the concentration of NADH. On the rGO modified electrode, the linear dynamic range is 2–300 μM, while on the MWNT modified electrode the linear dynamic range is 0.3–750 μM. The high sensitivity and quick and linear response of the electrodes to a wide concentration range of NADH indicates it is feasible to use the modified electrodes to trace the generation of NADH in the ADH enzymatic reaction system.

In addition, the modified electrodes showed good reproducibility for the amperometric measurements. Five replicated measurements of the same solutions with 3.0 and 150 μM of NADH gave a standard deviation of approximately 4% for the oxidation current. If five freshly made electrodes were used, the standard deviation of the measured currents was approximately 3%.

3.3. Measurements of the enzymatic activity of ADH in the absence and presence of Al^{3+} and nano-Al_{13}

The ADH enzyme system can be regarded as the major detoxifying machinery for alcohol and aldehyde. The conversion of ethanol to acetaldehyde is coupled with the reduction of NAD^+ to

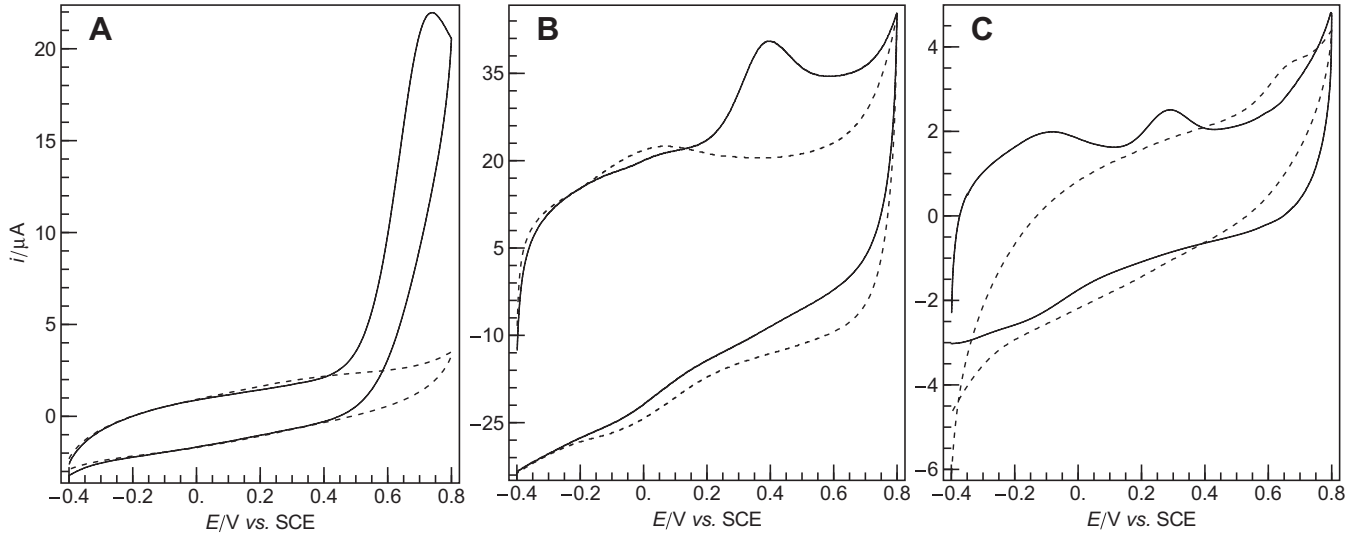

Fig. 1. Cyclic voltammograms obtained on the bare glassy carbon electrode (A and dashed curve in C), the reduced graphene oxide modified electrode (B) and the functionalised multi-walled carbon nanotube modified electrode (solid curve in C). (A and B) With (solid curve) and without (dashed curve) 1.5 mM NADH on the bare glassy carbon electrode (A) and the reduced graphene oxide modified electrode (B) in 0.1 M tris–HCl buffer solution (pH 7.5), scan rate 50 mV/s; (C) 0.3 mM NADH in 0.1 M tris–HCl buffer solution (pH 7.5) on the bare glassy carbon electrode (dashed curve) and the multi-walled carbon nanotube modified electrode (solid curve), scan rate 10 mV/s.

NADH. The reaction is important for many metabolic effects of ethanol (Lieber, 1999).

$$CH_3CH_2OH + NAD^+ \xrightarrow{ADH} CH_3CHO + NADH + H^+$$

The amperometric measurements using the modified electrodes were used to determine the enzymatically generated NADH in the absence and presence of ADH. The assay solutions included the oxidised form of the coenzyme, NAD^+. The amperometric response *i*–*t* curves are given in Fig. 2. For the solution with the substrate (ethanol) and NAD^+ only in the tris–HCl buffer, the *i*–*t* curves are essentially a straight line after the initial jump-up (see the grey curves in Fig. 2A and B). With the addition of 10 μL ADH (10 mg/mL) into the 5 mL assay solutions, the anodic oxidative current gradually increased with time (black curves in Fig. 2A and B). The amount of the newly generated NADH could be calculated from the increased magnitude of the current, and thus the enzymatic activity was measured. Particularly, during the first seconds after the addition of ADH, the current increased linearly with time. From the slope of the *i*–*t* curves, we could calculate the initial reaction rate, V_0.

The oxidation current of NADH catalytically converted from NAD^+ by ADH was measured in the presence of Al^{3+} and nano-Al_{13} in the above enzyme system. As shown in Fig. 2C and D, with the addition of 30 μM Al^{3+} (thin black curves) or nano-Al_{13} (thin grey curves) into the assay solutions, the oxidation current became smaller compared with the system without the Al(III) species (thick black curves). The results indicated the catalytic activity of ADH was slowed down by Al^{3+} and nano-Al_{13} and fewer NADH molecules were generated. Therefore, Al^{3+} and nano-Al_{13} are an inhibitor to the ADH enzyme-catalysed reaction. Moreover, the inhibitory effect of nano-Al_{13} on ADH was higher than that of the Al^{3+} species since the current decreased by a larger magnitude when the same concentration of nano-Al_{13} was added.

To obtain the kinetic parameters of the enzymatic reaction, the amperometric measurements were carried out in 5 mL 0.1 M tris–HCl buffer (pH 7.5) with a fixed concentration of 0.5 mM NAD^+, varied concentrations of ethanol and 0 or 30 μM Al^{3+} or nano-Al_{13}. The apparent Michaelis constant and the maximum reaction rate were calculated according to the classic Michaelis–Menten equation,

Table 1
The Michaelis constant (K_m) and the maximum rate (V_{max}) of the ADH enzyme system in the absence and presence of Al^{3+} and Al_{13} based on the amperometric measurements on the reduced graphene oxide modified electrode and the functionalised multi-walled carbon modified electrode. The measurements were carried out in 0.1 M tris–HCl buffer (pH 7.5) with a fixed concentration of 0.5 mM NAD^+.

Electrodes	Al(III)	K_m (μM)	V_{max} (μmol min^{-1})
Reduced graphene oxide modified electrode	No Al^{3+} or Al_{13}	627.3	0.485
	30 μM Al^{3+}	864.1	0.392
	30 μM Al_{13}	992.3	0.453
Functionalised multi-walled carbon nanotube modified electrode	No Al^{3+} or Al_{13}	580.8	0.412
	30 μM Al^{3+}	644.6	0.328
	30 μM Al_{13}	715.0	0.395

$$v = \frac{V_{max}[S]}{K_m + [S]}$$

where K_m is the Michaelis constant, v is the steady-state rate of the enzymatic reaction, [S] is the initial concentration of the substrate (ethanol), V_{max} is the limiting value of v at saturation concentrations of the substrate. The results are shown in Table 1. It shows that the apparent Michaelis constant of the enzyme system was 627.3 μM on the rGO modified electrode and 580.8 μM on the MWNT modified electrode in the absence of the Al(III) species. The kinetic values obtained on the two electrodes had larger differences in the presence of Al^{3+} and Al_{13}. The observed differences might be due to the interactions of the nanomaterials and the enzyme. More studies are needed to investigate this.

The initial reaction rates (V_0) were measured using the amperometric *i*–*t* curves after adding 10 μL ADH (10 mg/mL) into the 5 mL assay solutions of the enzymatic system with 1 mM ethanol and 1 mM NAD^+ in 0.1 M tris–HCl buffer at three different pH values. The measured dependence of V_0 on the concentration of Al^{3+} or Al_{13} at three pH conditions is shown in Fig. 3.

Although the initial reaction rate of ADH itself varied at different pH values, Fig. 3A and B shows that V_0 decreased most dramatically at pH 6.5, and this indicated that the inhibitory effect of Al^{3+} was strongest at acidic pH. At the elevated pH values, the effect decreased, which might be due to the hydrolysis of Al^{3+}. However,

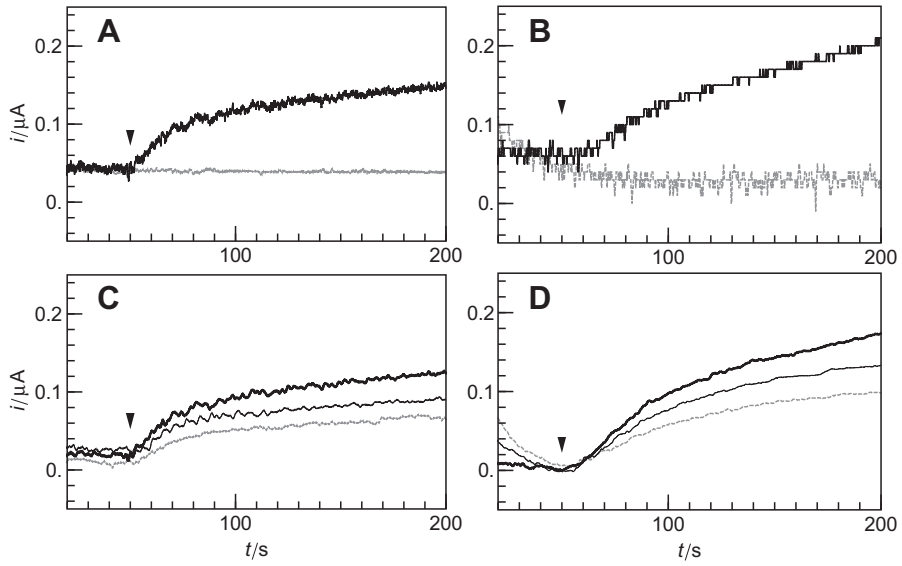

Fig. 2. Amperometric response current (*i*) versus time (*t*) curves on the reduced graphene oxide modified electrode (A and C) and the functionalised multi-walled carbon nanotube modified electrode (B and D) in 5 mL 0.1 M tris–HCl buffer (pH 7.5) solution with 2 mM ethanol and 0.5 mM NAD^+. (A and B) The thin grey curves were obtained in the solution system without adding the enzyme and the thick black curves were obtained in the solution system with 10 μL ADH (10 mg/mL) added at the time marked by the arrow; (C and D) the thick black, thin black and thin grey curves were obtained in the solution systems without adding Al(III) species, with 30 μM Al^{3+} and 30 μM Al_{13}, respectively, and 10 μL ADH (10 mg/mL) added at the time marked by the arrow.

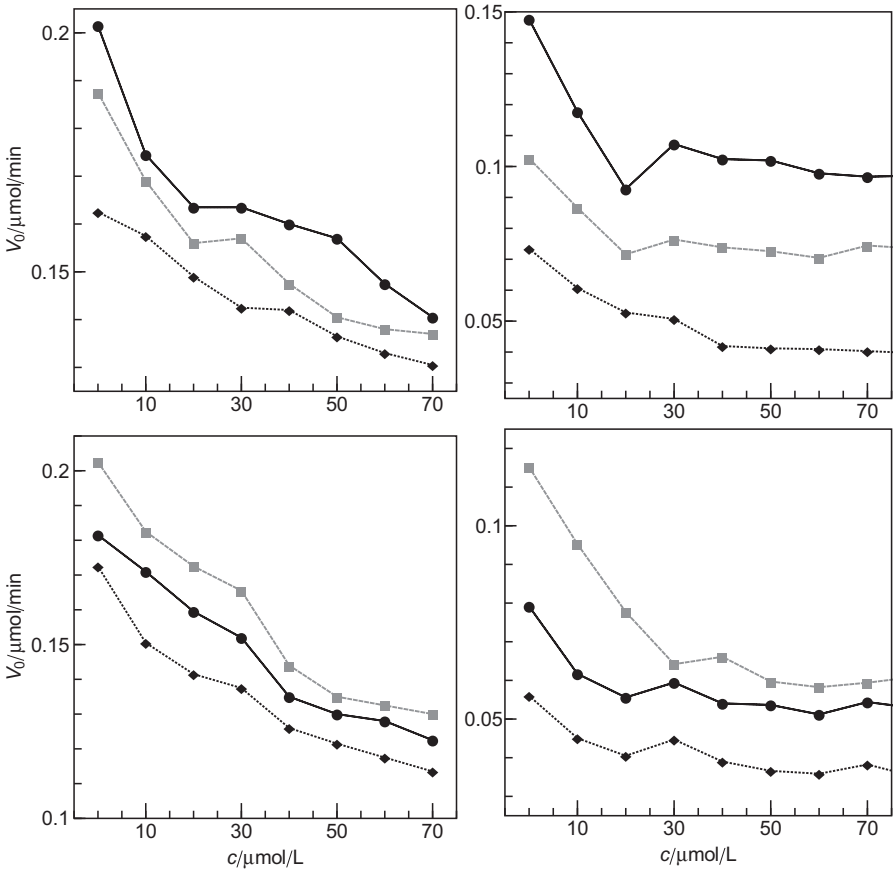

Fig. 3. Effect of Al^{3+} and Al_{13} on the initial reaction rate V_0 of the enzymatic catalytic reaction at different pH values measured on the graphene oxide modified electrode (A and C) and the functionalised multi-walled carbon nanotube modified electrode (B and D). The filled circle, square and diamond symbols represent the values obtained at pH 6.5, 7.5 and 8.5, respectively. The connected lines are to guide reader's eyes. The initial reaction rates (V_0) were measured using the amperometric *i–t* curves after adding 10 μL ADH (10 mg/mL) into the 5 mL assay solutions of the enzymatic system with 1 mM ethanol and 1 mM NAD^+ in 0.1 M tris–HCl buffer at specified pH values.

Fig. 3C and D shows that unlike Al^{3+} the inhibitory effect of Al_{13} was highest at nearly neutral pH 7.5. The phenomenon could be explained by the fact that the stability of Al_{13} varies with pH; it can stably exist around pH 7.5, whereas it may be depolymerised at pH 8.5 or 6.5 (Chen, Luan, Jia, & Li, 2009).

The exact mechanism of the inhibitory effect of the two aluminium species on the ADH enzymatic activity requires detailed studies at the molecular level. We conjectured that the major reason for the decrease of the ADH activity might be due to the significant conformational changes of NAD^+ and/or ADH induced by Al^{3+} and Al_{13}. A previous study (Yang et al., 2007) found that NAD^+ favoured the folded conformation upon complexation with Al(III) species, but the extending conformation was found at the catalytic side of ADH in the X-ray crystal structure (PDB ID: 2HCY). Fluorescence and circular dichroism (CD) spectra of ADH, given in Fig. 4, showed significant changes after the addition of Al^{3+} or Al_{13} and this result suggested significant conformational changes also occurred to ADH. Particularly, the far-UV region of the CD spectra, which reveals important characteristics of the secondary structure, indicated an alteration in the secondary structure of the enzyme. Thorough spectroscopic studies along with more detailed enzymatic kinetics studies using the electrochemical method developed here will be carried out in the future, in order to reveal how Al^{3+} and Al_{13} inhibit the activity of ADH and the implications for food chemistry and related fields.

Not all chemical species of aluminium are equivalently toxic. The amperometric measurements with the modified electrodes were also used to examine how Al(III) complexes with fluoride, citrate and oxalate affect the ADH activity. The curves of the initial reaction rate (V_0) versus the concentration of the complexes are given in the Supplemental Data. The results on both the modified electrodes indicated that the complexes of Al–F and Al–citrate had little effect on the activity of ADH, while the complex of Al–oxalate showed intermediate inhibitory effect. Free Al^{3+} and Al_{13}

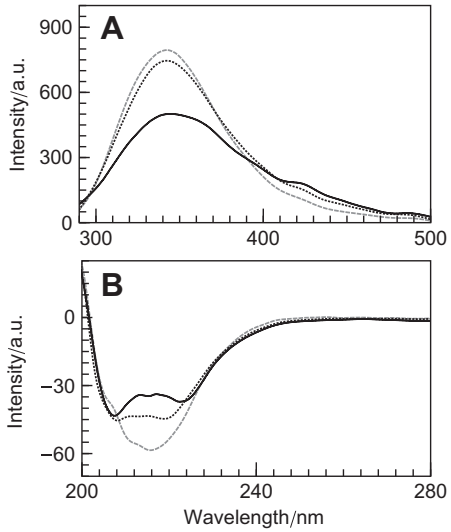

Fig. 4. Fluorescence emission spectra (A) and circular dichroism spectra (B) of 10 mg/mL ADH in the absence (grey dashed curve) and presence of 30 μM Al^{3+} (black dashed curve) or Al_{13} (black solid curve).

showed much more significant inhibitory effect in the parallel experiments.

4. Conclusions

We developed an electrochemical method to measure the enzymatic activity of NADH dependent enzymes using the modified glassy carbon electrodes. Both the reduced graphene oxide and the functionalised multi-walled carbon nanotube modified electrodes were effective in lowering the oxidation potential of NADH and the amperometric measurements had high sensitivity and wide linear dynamic range in detection of NADH. The amperometric measurements were successfully applied to determine the initial reaction rate, Michaelis constant and other kinetic parameters of the ADH reaction system. We also found that both Al^{3+} and Al_{13} exhibited inhibitory effect on the enzymatic activity of ADH and the inhibition of Al_{13} is stronger. Fluorescence and circular dichroism spectra showed that Al^{3+} and Al_{13} could induce conformational changes of ADH and NADH. However, more extensive experimental and theoretical studies are needed to investigate how the Al(III) species affect the enzymatic reaction kinetics and to learn the detailed interactions between the Al(III) species and the enzyme systems.

Acknowledgements

The project is supported by the National Natural Science Foundation of China (Grant No. 20875047), the research funding of Ministry of Water Resources (201201018) and the Priority Academic Program Development of Jiangsu Higher Education Institutions. XW acknowledges the financial support from the National Natural Science Foundation of China (21103016) and the Research Fund for the Doctoral Program of Higher Education of China (20100185120023).

Appendix A. Supplementary data

Supplementary data associated with this article can be found, in the online version, at http://dx.doi.org/10.1016/j.foodchem.2012.11.137.

References

Auger, C., Lemire, J., Cecchini, D., Bignucolo, A., & Appanna, V. D. (2011). The metabolic reprogramming evoked by nitrosative stress triggers the anaerobic utilization of citrate in *Pseudomonas fluorescens*. *PLoS One, 6*(12), e28468.

Cai, L., Xie, Y. F., Li, L., Li, H. H., Yang, X. D., & Liu, S. Q. (2010). Electrochemical and spectral study on the effects of Al(III) and nano-Al_{13} species on glutamate dehydrogenase activity. *Colloids and Surface. B, Biointerfaces, 81*(1), 123–129.

Casey, W. H. (2006). Large aqueous aluminum hydroxide molecules. *Chemical Reviews, 106*(1), 1–16.

Chen, Z. Y., Luan, Z. K., Jia, Z. P., & Li, X. S. (2009). On the acid-base stability of Keggin Al_{13} and Al_{30} polymers in polyaluminum coagulants. *Journal of Material Science, 44*(12), 3098–3111.

Copeland, L., & De Lima, M. L. (1992). The effect of aluminum on enzyme activities in wheat root. *Journal of Plant Physiology, 140*(6), 641–645.

Devi, P. G., Chakraborty, P. K., & Dasgupta, D. (2009). Inhibition of a Zn(II)-containing enzyme, alcohol dehydrogenase, by anticancer antibiotics, mithramycin and chromomycin A_3. *Journal of Biological Inorganic Chemistry, 14*(3), 347–359.

Exley, C., Price, N. C., & Birchall, J. D. (1994). Aluminum inhibition of hexokinase activity in vitro: a study in biological availability. *Journal of Inorganic Biochemistry, 54*(4), 297–304.

Furrer, G., Phillips, B. L., Ulrich, K. U., Pöthig, R., & Casey, W. H. (2002). The origin of aluminum flocs in polluted streams. *Science, 297*(5590), 2245–2247.

Gorton, L., & Domínguez, E. (2002). Electrocatalytic oxidation of NAD(P)H at mediator-modified electrodes. *Reviews in Molecular Biotechnology, 82*(4), 371–392.

Guzmán, K. A., Taylor, M. R., & Banfield, J. F. (2006). Environmental risks of nanotechnology: National Nanotechnology Initiative funding, 2000–2004. *Environmental Science and Technology, 40*(5), 1401–1407.

Hu, C. Z., Liu, H. J., & Qu, J. H. (2005). Preparation and characterization of polyaluminum chloride containing high content of Al_{13} and active chlorine. *Colloids and Surface. A, Physicochemical and Engineering Aspects, 260*(1–3), 109–117.

Kovtyukhova, N. I., Ollivier, P. J., Martin, B. R., Mallouk, T. E., Chizhik, S. A., Buzaneva, E. V., et al. (1999). Layer-by-layer assembly of ultrathin composite films from micron-sized graphite oxide sheets and polycations. *Chemistry Materials, 11*(3), 771–778.

Lieber, C. S. (1999). Microsomal ethanol-oxidizing system (MEOS): The first 30 years (1968–1998) – A review. *Alcoholism, Clinical and Experimental Research, 23*(6), 991–1007.

Lortie, R., Fassouane, A., Laval, J. M., & Bourdillon, C. (1992). Displacement of equilibrium in electroenzymatic reactor for acetaldehyde production using yeast alcohol dehydrogenase. *Biotechnology and Bioengineering, 39*(2), 157–163.

Ma, Q., Liu, T., Tang, T. T., Yin, H. S., & Ai, S. Y. (2011). Drinking water disinfection by hemin-modified graphite felt and electrogenerated reactive oxygen species. *Electrochimica Acta, 56*(6), 2748–2753.

Orihuela, D., Meichtry, V., & Pizarro, M. (2005). Aluminium-induced impairment of transcellular calcium absorption in the small intestine: Calcium uptake and glutathione influence. *Journal of Inorganic Biochemistry, 99*(9), 1879–1886.

Ramaswamy, S., Kratzer, D. A., Hershey, A. D., Rogers, P. H., Arnone, A., Eklund, H., et al. (1994). Crystallization and preliminary crystallographic studies of *Saccharomyces cerevisiae* alcohol dehydrogenase I. *Journal of Molecular Biology, 235*(2), 777–779.

Rao, G. V., & Rao, K. S. (1992). Evidence for a hydroxyl-aluminum polymer (Al_{13}) in synaptosomes. *FEBS Letters, 311*(1), 49–50.

Saleh, F. S., Rahman, M. R., Okajima, T., Mao, L., & Ohsaka, T. (2011). Determination of formal potential of NADH/NAD^+ redox couple and catalytic oxidation of NADH using poly(phenosafranin)-modified carbon electrodes. *Bioelectrochemistry, 80*(2), 121–127.

Sánchez-Iglesias, S., Méndez-Alvarez, E., Iglesias-González, J., Muñoz-Patiño, A., Sánchez-Sellero, I., Labandeira-García, J. L., et al. (2009). Brain oxidative stress and selective behaviour of aluminum in specific areas of rat brain: Potential effects in a 6-OHDA-induced model of Parkinson's disease. *Journal of Neurochemistry, 109*(3), 879–888.

Shi, B. Y., Li, G. H., Wang, D. S., & Tang, H. X. (2007). Separation of Al_{13} from polyaluminum chloride by sulfate precipitation and nitrate metathesis. *Separation and Purification Technology, 54*(1), 88–95.

Soni, M. G., White, S. M., Flamm, W. G., & Burdock, G. A. (2001). Safety evaluation of dietary aluminum. *Regulatory Toxicology and Pharmacology, 33*(1), 66–79.

Wang, J., Yang, S., Guo, D., Yu, P., Li, D., Ye, J., et al. (2009). Comparative studies on electrochemical activity of graphene nanosheets and carbon nanotubes. *Electrochemistry Communications, 11*(10), 1892–1895.

Yang, X. D., Li, L. F., & Bi, S. P. (2005). Electrochemical studies of the inhibition and activation effects of Al(III) on the activity of bovine liver glutamate dehydrogenase. *Sensors, 5*(4), 235–244.

Yang, X. D., Zhang, Q. Q., Li, L. F., & Shen, R. F. (2007). Structural features of aluminium(III) complexes with bioligands in glutamate dehydrogenase reaction system – A review. *Journal of Inorganic Biochemistry, 101*(9), 1242–1250.

Yin, G. W., Wei, W., Xu, J., Li, Z. F., Wang, B. H., & Du, W. H. (2010). Interaction of Nickel(II) with yeast alcohol dehydrogenase. *Acta Physico-Chimica Sinica, 26*(4), 1107–1112.

Yuan, J. H., Chen, J. R., Wu, X. H., Fang, K. M., & Niu, L. (2011). A NADH biosensor based on diphenylalanine peptide/carbon nanotube nanocomposite. *Journal of Electroanalytical Chemistry, 656*(1–2), 120–124.

Zhou, M., Zhai, Y. M., & Dong, S. J. (2009). Electrochemical sensing and biosensing platform based on chemically reduced graphene oxide. *Analytical Chemistry, 81*(14), 5603–5613.

Zhu, J., Chen, X., & Yang, W. S. (2010). A high performance electrochemical sensor for NADH based on graphite nanosheet modified electrode. *Sensors and Actuators. B, Chemical, 150*(2), 564–568.